



HAL
open science

Spectroscopic analysis of keratin endogenous signal for skin multiphoton microscopy

Ana-Maria Pena, Mathias Strupler, Thierry Boulesteix, Marie-Claire Schanne-Klein

► **To cite this version:**

Ana-Maria Pena, Mathias Strupler, Thierry Boulesteix, Marie-Claire Schanne-Klein. Spectroscopic analysis of keratin endogenous signal for skin multiphoton microscopy. *Optics Express*, 2005, 13 (16), pp.6268-6274. 10.1364/OPEX.13.006268 . hal-00807874

HAL Id: hal-00807874

<https://polytechnique.hal.science/hal-00807874v1>

Submitted on 15 May 2014

HAL is a multi-disciplinary open access archive for the deposit and dissemination of scientific research documents, whether they are published or not. The documents may come from teaching and research institutions in France or abroad, or from public or private research centers.

L'archive ouverte pluridisciplinaire **HAL**, est destinée au dépôt et à la diffusion de documents scientifiques de niveau recherche, publiés ou non, émanant des établissements d'enseignement et de recherche français ou étrangers, des laboratoires publics ou privés.

Spectroscopic analysis of keratin endogenous signal for skin multiphoton microscopy

A.-M. Pena, M. Strupler, T. Boulesteix, and M.-C. Schanne-Klein

Laboratory for Optics and Biosciences, CNRS/INSERM, Ecole Polytechnique, 91128 Palaiseau cedex, FRANCE
marie-claire.schanne-klein@polytechnique.fr

Abstract: We recorded one-photon excited fluorescence (1PEF) and two-photon excited fluorescence (2PEF) spectra of purified keratin from human epidermis, and determined the action cross section of this endogenous chromophore. We used this spectroscopic analysis to analyse multiphoton images of skin biopsies and assign the intrinsic fluorescence signals in the epidermis. We observed a good agreement between *in situ* and *in vitro* 2PEF spectra of keratin. This study provides a comprehensive characterization of the 2PEF signal of the keratins from the epidermis, and will be of practical interest for multiphoton imaging of the skin.

©2005 Optical Society of America

OCIS codes: 170.2520 (fluorescence microscopy); 170.6510 (Spectroscopy, tissue diagnosis); 190.4180 (multiphoton processes)

References and links

1. W. Denk, J. H. Strickler and W. W. Webb, "Two-photon laser scanning microscopy," *Science* **248**, 73-76 (1990)
2. B. R. Masters, P. T. C. So and E. Gratton, "Multiphoton excitation fluorescence microscopy and spectroscopy of in vivo human skin," *Biophys. J.* **72**, 2405-2412 (1997)
3. K. König and I. Riemann, "High-resolution multiphoton tomography of human skin with subcellular spatial resolution and picosecond time resolution," *J. Biomed. Opt.* **8**, 432-439 (2003)
4. G. Cox, E. Kable, A. Jones, I. Fraser, K. Marconi and M. D. Gorrell, "3-dimensional imaging of collagen using second harmonic generation," *J. Struct. Biol.* **141**, 53-62 (2003)
5. C.-K. Sun, C.-C. Chen, S.-W. Chu, T.-H. Tsai, Y.-C. Chen and B.-L. Lin, "Multiharmonic-generation biopsy of skin," *Opt. Lett.* **28**, 2488-2490 (2003)
6. L. Coghlan, U. Utzinger, R. Drezek, D. Heintzelman, A. Zuluaga, C. Brookner and R. Richards-Kortum, "Optimal fluorescence excitation wavelengths for detection of squamous intra-epithelial neoplasia: results from an animal model," *Opt. Express* **7**, 436-446 (2000)
7. L. Brancalion, A. J. Durkin, J. H. Tu, G. Menaker, J. D. Fallon and N. Kollias, "In vivo fluorescence spectroscopy of nonmelanoma skin cancer," *Photochem. Photobiol.* **73**, 178-183 (2001)
8. D. C. G. D. Veld, M. Skurichina, M. J. H. Witjes, R. P. W. Duin, H. J. C. M. Sterenborg and J. L. N. Roodenburg, "Clinical study for classification of benign, dysplastic, and malignant oral lesions using autofluorescence spectroscopy," *J. Biomed. Opt.* **9**, 940-950 (2004)
9. Y. Wu, P. Xi, J. Y. Qu, T. H. Cheung and M. Y. Yu, "Depth-resolved fluorescence spectroscopy of normal and dysplastic cervical tissue," *Opt. Express* **13**, 382-388 (2005)
10. R. A. Davis, H. E. Savage, P. G. Sacks, R. R. Alfano and S. P. Schantz, "The influence of keratin on native cellular fluorescence of human skin," in *Advances in Laser and Light Spectroscopy to Diagnose Cancer and Other Diseases III: Optical Biopsy*, R. R. Alfano and A. Katzir, Eds., Proc. SPIE 2679, 216-226 (1996)
11. Y. Wu, P. Xi, J. Y. Qu, T. H. Cheung and M. Y. Yu, "Depth-resolved fluorescence spectroscopy reveals layered structure of tissue," *Opt. Express* **12**, 3218-3223 (2004)
12. R. M. Porter and E. B. Lane, "Phenotypes, genotypes and their contributions to understanding keratin function," *Trends in Genetics* **19**, 278-285 (2003)
13. R. Eichner and M. Kahn, "Differential extraction of keratin subunits and filaments from normal human epidermis," *J. Cell Biol.* **110**, 1149-1158 (1990)
14. C. Xu and W. W. Webb, "Measurement of two-photon excitation cross sections of molecular fluorophores with data from 690 to 1050 nm," *J. Opt. Soc. Am. B* **13**, 481-491 (1996)
15. T. Boulesteix, E. Beaupaire, M.-P. Sauviat and M. C. Schanne-Klein, "Second harmonic microscopy of unstained living cardiac myocytes: measurements of sarcomere length with 20 nm accuracy," *Opt. Lett.* **29**, 2031-2033 (2004)

16. D. Débarre, W. Suppato, E. Farge, B. Moulia, M. C. Schanne-Klein and E. Beaufort, "Velocimetric third-harmonic generation microscopy: micrometer-scale quantification of morphogenetic movements in unstained embryos," *Opt. Lett.* **29**, 28881-28884 (2004)
 17. L. Moreaux, O. Sandre, M. Blanchard-Desce and J. Mertz, "Membrane imaging by simultaneous second-harmonic generation and two-photon microscopy," *Opt. Lett.* **25**, 320-322 (2000)
 18. W. R. Zipfel, R. M. Williams, R. Christie, A. Y. Nikitin, B. T. Hyman and W. W. Webb, "Live tissue intrinsic emission microscopy using multiphoton-excited native fluorescence and second harmonic generation," *Proc. Natl. Acad. Sci. USA* **100**, 7075-7080 (2003)
 19. C. Buehler, K. H. Kim, U. Greuter, N. Schlumpf and P. T. C. So, "Single-photon counting multicolor multiphoton fluorescence microscope," *J. Fluorescence* **15**, 41-51 (2005)
 20. Z. Deyl, K. Macek, M. Adam and Vancikova, "Studies on the chemical nature of elastin fluorescence," *Biochim. Biophys. Acta* **625**, 248-254 (1980)
 21. R. Richards-Kortum and E. Sevick-Muraca, "Quantitative optical spectroscopy for tissue diagnosis," *Annu. Rev. Phys. Chem.* **47**, 555-606 (1996)
 22. T. G. Scott, R. D. Spencer, N. J. Leonard and G. Weber, "Emission properties of NADH. Studies of fluorescence lifetimes and quantum efficiencies of NADH, AcPyADH and simplified synthetic models," *J. Am. Chem. Soc.* **92**, 687-695 (1969)
-

1. Introduction

Since its first demonstration in 1990 [1], multiphoton microscopy has appeared as a valuable tool to image the skin, which is particularly accessible to optical techniques [2-5]. Skin contains several endogenous fluorophores, notably elastin, NADH, flavoproteins or keratin, which can be excited by two-photon absorption and provide a strong two-photon excited fluorescence (2PEF) signal. It can be combined with the second harmonic generation (SHG) signal by the fibrillar collagen in the dermis, so that simultaneous 2PEF/SHG microscopy provides a powerful imaging technique of the skin up to 200 μm depth typically. A particularly exciting application of this new technique would be the detection of skin pathologies. Variations of the skin intrinsic fluorescence in different lesions have indeed been demonstrated using confocal microscopy studies [6-9].

However, satisfactory implementation of multiphoton microscopy lacks a complete characterization of the endogenous chromophores in the skin. In particular, while several groups have studied the 2PEF signal from elastin, NADH or flavoproteins, the spectroscopic properties of the keratin have been poorly characterized and no 2PEF spectrum of the purified protein has been reported yet. Fluorescence signals from the epidermis were already attributed to this protein on the basis of histological localisation [3,10,11]. The epidermis contains different keratin types [12] secreted by the keratinocytes which represent 90% of the epidermal cells. Newly formed cells are slowly pushed to the surface and as they move from one epidermal layer to the next one they accumulate more and more keratin, a process called keratinisation, so that the upper layers of the epidermis become completely keratinized. This allows for a direct *in situ* spectral analysis of the keratin fluorescence from histological skin samples, with negligible contribution from other endogenous fluorophores.

In the following, we present a complete characterisation of the keratin fluorescence signal, including optical linear and nonlinear spectroscopy and multiphoton microscopy experiments. We performed *in vitro* spectroscopic experiments and measured one-photon-excited fluorescence (1PEF), two-photon-excited fluorescence (2PEF) and action cross section on purified keratin solution. We then compared these results to 2PEF spectra acquired *in situ* from histological human skin samples performing multiphoton microscopy experiments.

2. Materials and methods

2.1 Keratin and skin samples

Purified keratin from human epidermis [13] was purchased from Sigma-Aldrich as a 30mg/ml solution in urea (product K0253, solution in 8 M urea, 50 mM Tris, 0.1 M β -mercaptoethanol and 0.1% sodium azide). The purification process resulted in a mixture of various cytokeratins as illustrated by the electrophoresis analysis showing several bands in the 45 to 60 kDa range. The keratin solution was studied in a 100 μm optical path fused silica microcell (QS-106,

Hellma). Thin histological cuts were obtained from human normal skin biopsies fixed in 10% buffered formalin and embedded in paraffin.

2.2 Optical spectroscopy

Linear spectroscopic characterizations were performed using a CARY 500 spectrophotometer (Varian) and a Hitachi F-4500 spectrofluorimeter. 2PEF spectra were recorded using a custom-built 2-photon spectrofluorimeter as represented on Fig. 1. Light excitation was provided by a femtosecond Titanium-sapphire laser, tunable in the 700-1000 nm range (Tsunami, Spectra-Physics). The laser intensity was controlled through a half waveplate followed by a Glan prism. The laser beam was expanded through an afocal combination of 2 lenses in order to ensure filling of the back aperture of a 20x, 0.4 NA IR objective (Olympus) and to precisely define the excitation volume in the cell. The fluorescence was collected by the same objective and directed by a dichroic mirror (700DCXRU, Chroma) onto a photomultiplier tube (H5783P, Hamamatsu). In order to measure 2PEF cross sections or excitation spectra, the setup efficiency was calibrated with a fluorescein solution (pH=11, concentration 5.5 $\mu\text{mol/L}$) using the data published by Xu and Webb [14]. We also measured an absolute fluorescein excitation spectrum, by correcting our data for the variations of the laser pulses characteristics and the variations of the detector and optical components transmissions when tuning the laser wavelength. We obtained a good agreement with the fluorescein spectrum reported in ref [14]. Finally, we inserted a monochromator (H10, Jobin Yvon) on the fluorescence path in order to measure 2PEF spectra at fixed excitation wavelength.

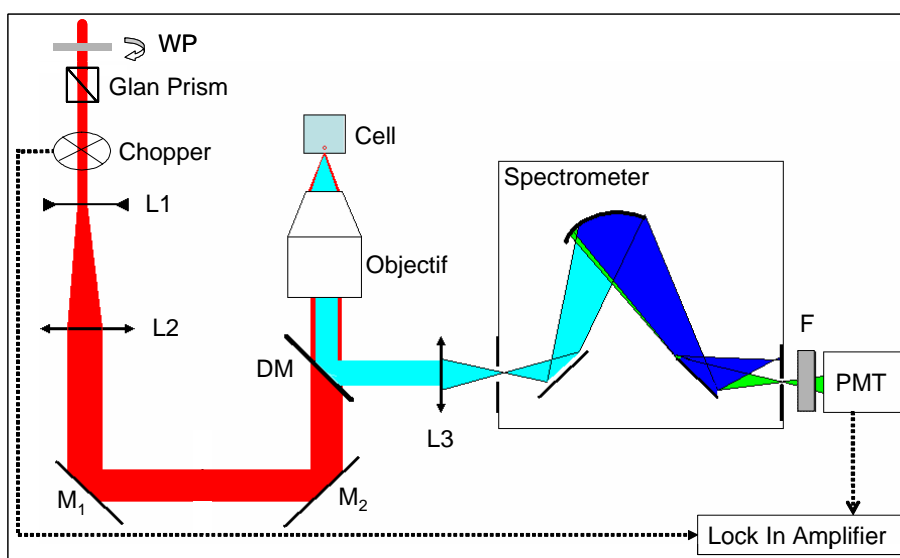


Fig. 1. 2-photon spectrofluorimeter. WP: rotating half waveplate; L1, L2, L3: lenses; M₁, M₂: silver mirrors; DM: dichroic mirror; F: optical filters; PMT: photomultiplier tube.

2.3 Laser scanning multiphoton microscope

Combined 2PEF/SHG imaging was performed using a custom-built laser scanning microscope incorporating a femtosecond Titanium-sapphire laser (Mira, Coherent), galvanometer mirrors (GSI Lumonics) and photon-counting photomultiplier modules (Electron Tubes) [15, 16]. Detection channels were implemented both in the reflected and transmitted directions, to allow for simultaneous detection of 2PEF and SHG signals using appropriate filters [17]. We used a 20 \times , 0.95-NA objective lens (Olympus) in order to combine a large field of view and a high spatial resolution. In the experiments reported here, the objective back aperture was

underfilled, resulting in 0.8 effective excitation N.A.. Thin histological cuts were usually illuminated with a few mW average power, which resulted in no visible laser-induced morphological alterations. The excitation power was increased up to 25 mW when recording spectra, and we observed a decrease of the signal of 15% maximum after 8 minutes acquisition.

In the spectral studies, we used a tunable interferential filter (S-60, Schott) on the backward channel, with the following characteristics: 6.6 nm/mm reciprocal linear dispersion, 15 nm FWHM (full width at half maximum) and 30-50 % peak transmission. We shifted slightly the filter in order to tune the transmitted wavelength and recorded stacks of images corresponding to different spectral components. The filter was inserted on a descanned path, utilizing a dichroic mirror before the galvanometric mirrors, and the spectral response of this detection path was calibrated using retinol fluorescence [18]. We measured an effective FWHM of the tunable filter of about 20 nm, as given by the FWHM of the SHG peak arising from collagen fibers. We recorded simultaneously the full fluorescence signal in the forward channel in order to correct for any decrease of the signal during acquisition of the stacks.

3. Spectroscopic characterization of keratin

3.1 Linear spectroscopy

The 1-photon absorption (1PA) and fluorescence (1PEF) spectra of the keratin solution are displayed on Fig. 2(a). The keratin solution exhibits a first absorption peak at 277 nm, with a 30 nm FWHM, which is characteristic for aromatic amino-acids, and a second peak around 210 nm, which corresponds to the protein backbone absorption. Excitation of the keratin solution at 277 nm results in fluorescence peaking at 382 nm, with a 50 nm FWHM. No fluorescence was observed when exciting at 214 nm.

3.2 Keratin 2PEF spectra

Looking at the linear optical properties of the keratin solution, one expects 2-photon absorption (2PA) to occur around 544 nm which is out of the Ti-Sa range. Conversely, 3-photon absorption (3PA) is expected around 831 nm and the keratin fluorescence observed in multiphoton microscopy may be due to 3PA. However, 2PA spectra may exhibit wider peaks than 1PA spectra due to different selection rules and 2PA of keratin may extend to the Ti-Sa range. To verify that point, we measured the fluorescence intensity as a function of the excitation intensity at 800 nm and plotted our results in a log-log scale as displayed on Fig. 2(b). Fitting our data resulted in a 1.91 ± 0.06 slope in good agreement with a quadratic dependency, considering the uncertainty on the power measurements. It indicates unambiguously a quadratic process and proves that we observed the 2PEF of the keratin solution. We also verified that the urea buffer solution in which keratin was dissolved presented no 2PEF signal. However, the Ti-Sa wavelength range is not optimized to excite the keratin 2PEF, as indicated by Fig. 2(c). Looking at the fluorescence spectra of the keratin solution excited at various wavelengths in the Ti-Sa range, the fluorescence peak shifts linearly towards smaller wavelengths when decreasing the excitation wavelength. Even at 750 nm excitation, fluorescence occurs at higher wavelengths than in the 1PEF spectrum displayed on Fig. 2(a), because it is Stokes shifted compared to the excitation harmonic at 375 nm. We did not try to optimize the keratin 2PEF using a blue shifted excitation source and to analyze the keratin 2PEF spectral position and width, because we are specifically interested in characterizing the keratin fluorescence for multiphoton microscopy applications using Ti-Sa excitation. Our experiments aimed at determining whether keratin exhibits 2PEF when excited around 800 nm, and our results clearly demonstrate that it is the case.

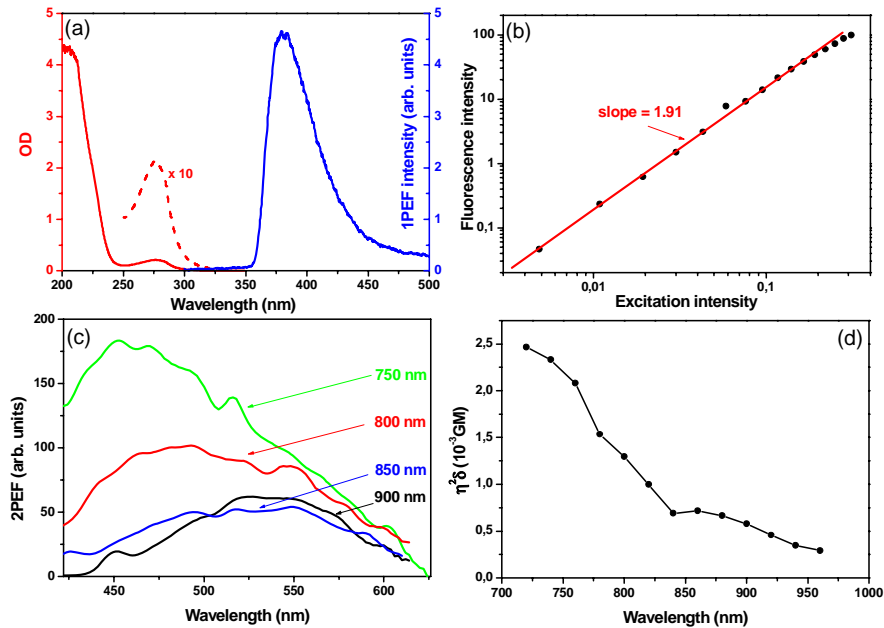


Fig. 2. spectroscopic analysis of the keratin solution in a 100 μ m optical path fused silica microcell (a): absorption and fluorescence spectra. (b): intensity dependence of the fluorescence signal upon Ti-Sa excitation at 800 nm; the red line correspond to an exponential fit of the experimental data (solid circles). (c) 2PEF spectra recorded at various excitation wavelengths, normalized to the same excitation intensity. (d) 2PEF excitation spectrum; error bar are typically $\pm 20\%$, and the absolute scale is determined within a 37% uncertainty.

3.3 Keratin 2PEF excitation spectra

Figure 2(d) shows the 2PEF excitation spectrum of the keratin solution. We normalized the fluorescence signal of the keratin by the one of the fluorescein measured in the same experimental conditions at every wavelength, and used the absolute value of the fluorescein cross section determined by Xu and Webb [14] to calibrate our data. We directly measured the action cross section of the keratin solution, $\eta_2\delta$, where δ is the 2PA cross section and η_2 the fluorescence quantum efficiency. This action cross section must be considered as an average value over the various types of keratin present in the solution. It is determined with a $\pm 42\%$ error, including the uncertainty on the molar concentration of the keratin solution due to the mixture of proteins of different masses and the uncertainty of the reference value reported in ref. [14].

The keratin action cross section increases when decreasing the laser wavelength and the 2PEF excitation spectrum peaks presumably at wavelengths smaller than 700 nm, as expected from the 1PA spectrum. The value measured in the Ti-Sa range is a few 10^{-3} GM (10^{-50} cm⁴ s/photon), which is much less than the action cross section of fluorescein (a few 10 GM) or other exogenous chromophores. Practically, it has the same order of magnitude as the 2PEF action cross section measured for other endogenous chromophores such as NADH, folic acid or cholecalciferol, although smaller than for the riboflavin [18].

4. In situ characterization of keratin 2PEF signal

4.1 Multiphoton imaging of skin histological cuts

Figure 3(a) shows a typical multiphoton image of a thin histological cut from 30 years aged human skin. 2PEF (red color) and SHG (green color) were acquired simultaneously in both channels of the microscope upon 860 nm excitation: 2PEF was selected using a GG455 (Schott) highpass filter and SHG was detected through an interferential filter HQ430/20 at the harmonic frequency. According to morphological considerations, we attributed the 2PEF signal observed in the upper layers of the epidermis to keratin, and the one in the skin dermis to elastic fibers. The SHG signal arises from the fibrillar collagen (essentially collagen I) found in the dermis.

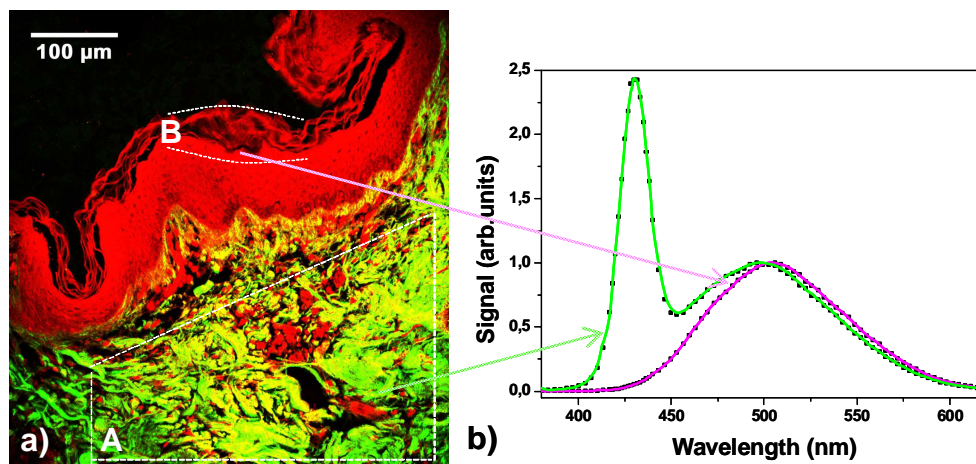


Fig. 3. skin multiphoton imaging and spectroscopic analysis (a) combined 2PEF (red) and SHG (green) image of a thin histological cut from human normal skin biopsy (b) spectra recorded in relevant areas with the tunable interferential filter (see table 1).

Table 1. 2PEF spectral positions in various skin areas

Excitation wavelength	760 nm	860 nm	Attribution
A Area	471 ± 3 nm	496 ± 3 nm	Elastin (and collagen SHG)
B Area	477 ± 3 nm	503 ± 3 nm	Keratin
Keratin solution	475 ± 5 nm	515 ± 5 nm	

4.2 In situ skin 2PEF spectra

We acquired fluorescence spectra in 2 relevant areas in the skin sample: the spectra on Fig. 3(b) correspond to the signal through the tunable interferential filter averaged over the areas displayed on Fig. 3(a). As expected from the combined 2PEF/SHG image on Fig. 3(a), the spectrum of the signal acquired in the dermis (area A) comprises a SHG component due to fibrillar collagen and a 2PEF component that we attributed to elastic fibers. We used the SHG peak generated by the fibrillar collagen as a spectral reference for all our spectra. Conversely, the spectra acquired in the epidermis exhibit only a wide peak, characteristic for fluorescence signal. Remarkably, the 2 fluorescence spectra exhibit slight but significant differences in the peak positions. We obtained similar results for 760 nm excitation (data not shown). Table 1 summarizes the spectral positions of the fluorescence peaks measured in these areas and in the keratin solution upon 760 and 860 nm excitation. The spectral position of the fluorescence peaks shifts towards smaller wavelengths when decreasing the excitation wavelength, as

already observed in the keratin solution. It similarly indicates that the excitation wavelength is not optimized to excite these endogenous chromophores.

5. Discussion

Let us now consider the 2PEF spectra recorded in the different skin areas. In the dermis area, the measured spectrum is in qualitative agreement with spectra already recorded in elastic fibers from human skin [18,19]. We also recorded the 2PEF spectrum of elastin powder from human aorta (product E6777, Sigma-Aldrich) at 760 nm excitation and measured a fluorescence peak around 445 nm (data not shown), in reasonable agreement with the 471 nm value in the skin tissue. We attribute the spectral discrepancy to differences in the tissues, as fluorescence spectra from elastin powder [20,21] or tissues [18,19] published in the literature seemed to vary significantly in different samples.

The stratified structures observed in Fig. 3(a) are characteristic for keratinized upper layers of the epidermis, so that we expected to measure the keratin fluorescence spectrum in this area. The fluorescence spectra we measured *in situ* are indeed similar to the spectra recorded in the keratin solution. Remarkably, we obtain a reasonable agreement for the peak positions, taking into account that the keratin fluorescence may be sensitive to the protein environment in the tissue or to the denaturation in the urea solution where the purified keratin was solubilized. Conversely, other sources of endogenous fluorescence such as NADH, melanin, or flavoproteins appear to be negligible here, probably due to the preparation method of the tissue. Other studies are needed on various samples to verify that point. However, our data show unambiguously that the endogenous fluorescence observed in the upper layers of the epidermis arises from keratin.

6. Conclusion

In summary, we studied the fluorescence properties of the keratin from the human epidermis. We report the first comparative 1PEF and 2PEF spectra of purified keratin, along with its estimated action cross section when excited in the Ti-Sa wavelength range. We performed multiphoton microscopy of skin histological cuts and used our spectroscopic characterization to assign *in situ* spectra recorded in various areas of the skin to different chromophores. We observed slight but reproducible spectral differences between various endogenous chromophores in epithelial tissue. These data will be of practical interest for the development of skin multiphoton histology applications.

Acknowledgments

The authors thank G. Godeau (Paris V University) for providing them with the skin histological cuts, and E. Beaufrepaire, D. Débarre and F. Hache for critical comments. This work was supported by Centre National de la Recherche Scientifique (CNRS), Institut National de la Santé et de la Recherche Médicale (INSERM) and Ecole Polytechnique.